



Heterometal functionalization yields improved energy density for charge carriers in nonaqueous redox flow batteries

Journal:	<i>Journal of Materials Chemistry A</i>
Manuscript ID	TA-ART-04-2018-003312.R2
Article Type:	Paper
Date Submitted by the Author:	25-Jun-2018
Complete List of Authors:	VanGelder, Lauren; University of Rochester, Department of Chemistry Matson, Ellen; University of Rochester, Chemistry



Heterometal functionalization yields improved energy density for charge carriers in nonaqueous redox flow batteries

Lauren E. VanGelder^a and Ellen M. Matson ^{*a}

Received 00th January 20xx,
Accepted 00th January 20xx

DOI: 10.1039/x0xx00000x

www.rsc.org/

The development of facile, high-yielding synthetic routes to energy-dense charge carriers is critical for the success of redox flow battery technologies. Here, we present the results of synthetic modifications to our recently established series of polyoxovanadium clusters, $[V_6O_7(OR)_{12}]$ ($R = CH_3, C_2H_5$), with respect to their performance as charge carriers for nonaqueous redox flow batteries. We demonstrate that incorporation of one ($[TiV_5(OCH_3)_{13}]^-$) or two ($[Ti_2V_4(OCH_3)_{14}]$) titanium ions within the Lindqvist core significantly increases the cell voltage of the system (from 1.60 V, to 2.30 and 2.74 V, respectively) while the solubility and redox stability observed for cluster complexes is retained. The improved physicochemical properties result in a 740% increase in energy density for $[TiV_5O_6(OCH_3)_{13}]^-$, and a 210% increase for $[Ti_2V_4O_5(OCH_3)_{14}]$. The kinetic implications of heterometal incorporation are assessed, demonstrating the importance of considering diffusion coefficients and heterogeneous electron transfer rate constants in mixed-metal charge carrier schematics. Ultimately, these results provide insight into structure-function relationships that will inform future synthetic design strategies of charge carriers for nonaqueous energy storage.

Introduction

The global effort to integrate intermittent renewable energy sources into the electrical grid has created a pressing need for the development of new electrochemical energy storage (EES) technologies.^{1,2} In particular, redox flow batteries (RFBs) have seen renewed interest, owing to the unique modularity and scalability of these systems.^{3,4} Yet despite these advantageous features, the low energy densities of current RFB charge carriers precludes their widespread application.^{5,6} To address this issue, alternative redox flow-based technologies have been explored, such as those using deep eutectic solvents⁷⁻⁹ or redox-targeting reactions.^{10,11} Alternative approaches to improving the energy density of RFBs have focused on improving the electrochemical and physical properties of relevance in a *molecular* charge carrier, as described by the equation:

$$\hat{E} = \frac{1}{2} n V_{cell} C_{active} F \quad (1)$$

Where \hat{E} is the volumetric energy density, n is the number of electrons transferred, V_{cell} is the average cell voltage, C_{active} is the concentration of active species, and F is Faraday's constant.¹²

The competition to improve RFB energy density has resulted in an increased focus on the design of charge carriers that are physically and electrochemically compatible with organic solvents.^{13,14} The broad potential window of nonaqueous media allows for expansion of V_{cell} without competing oxidative or

reductive degradation of solvent. To date, several molecular candidates for charge carriers in nonaqueous redox flow batteries (NRFBs) have been reported, including metal coordination complexes,¹⁵⁻²⁷ organic compounds,²⁸⁻³³ and redox-active polymers.³⁴⁻³⁷ Developments within this library of redox agents have focused on the identification of molecules that can be synthetically tuned, resulting in the modulation of physicochemical properties relevant to NRFB energy density (i.e. multi-electron transfer, redox potentials, and solubility). Indeed, in these examples, effective molecular improvements have been demonstrated through organic functionalization or metal substitution.^{15, 19-22, 24, 38-40} While these results have been promising, limitations in the solubility and/or stability of existing charge carriers drives the search for new electroactive materials for NRFBs.

Polyoxometalates have emerged as an attractive class of compounds for applications in energy storage technologies, due to their facile synthesis and fascinating electronic properties (Figure 1).⁴¹⁻⁴⁴ The compatibility of these highly charged, metal-oxide clusters with aqueous media has led to their use in a variety of water-based EES technologies.⁴⁵⁻⁵⁰ In contrast, the use of polyoxoanions in nonaqueous devices has been limited due to their low solubility and lack of electrochemical reversibility in organic solvents.^{50, 51} Recently, our research group has extended the investigation of POMs as charge carriers for NRFBs through the analysis of a series of hexavanadate, polyoxovanadate-alkoxide (POV-alkoxide) clusters, $[V_6O_7(OR)_{12}]$ ($R = CH_3, C_2H_5$).⁵² We established that incorporation of bridging alkoxide ligands improves the physicochemical properties of the system—not only by solubilizing the cluster in organic solvents, but also through the stabilization of the four reversible redox events of the mixed-

^a Department of Chemistry, University of Rochester, Rochester, NY 14627, USA.

*E-mail: matson@chem.rochester.edu

Electronic Supplementary Information (ESI) available: See DOI: 10.1039/x0xx00000x

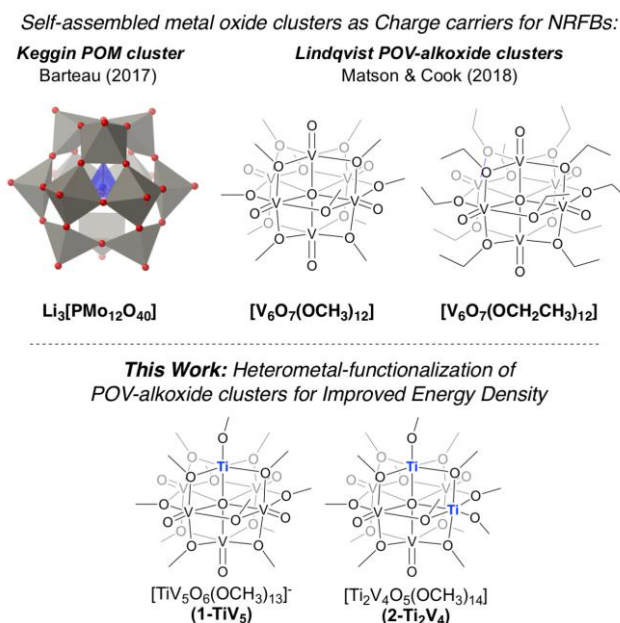


Figure 1. Self-assembled metal oxide clusters as charge carriers for non-aqueous redox flow batteries.⁵¹⁻⁵²

valent, Lindqvist core. This report marked a new direction for nonaqueous charge carrier development, focused on the use of self-assembled cluster complexes as multielectron electroactive materials for symmetric cells. The promising stability of the homometallic compound prompted investigations into molecular approaches to further improve the energy density of the system.

Herein, we report the development of heterometallic POV-alkoxide clusters as charge carriers for NRFBs. The use of a single, mixed-metal charge carrier with widely spaced redox events allows for the exploitation of benefits associated with a symmetric system, including resistance to degradative crossover processes. We demonstrate that substitution of d^0 metal centres within the Lindqvist core is an effective method for increasing the V_{cell} of the system, while retaining the characteristic electrochemical reversibility and stability of the POV-alkoxide in organic solvent. We assess the capability of these heterometallic clusters to serve as NRFB charge carriers through cyclic voltammetry, bulk electrolysis, and H-cell charge-discharge experiments. These results further highlight the modularity of the POV-alkoxide cluster series, and demonstrate the potential for heterometal incorporation to significantly improve the energy density of these NRFB charge carriers.

Results and discussion

Physical and Electronic Properties of TiPOV-alkoxide Clusters

Electrochemical analysis via cyclic voltammetry. Research in our laboratory is broadly focused on heterometal functionalization of POV-alkoxide clusters, for the purpose of exploiting the rich redox profiles of the Lindqvist core. We have reported synthetic routes for the installation of iron, titanium,

zirconium, and hafnium ions within the POV-alkoxide scaffold, demonstrating that heterometal identity has significant bearing on the redox potentials of the reversible $\text{V}^{\text{IV}}/\text{V}^{\text{V}}$ couples (Figure 2, Table 1).^{53, 54} In the case of the titanium-functionalized POV-alkoxide (TiPOV-alkoxide) cluster, $[\text{Ti}^{\text{IV}}\text{V}_5\text{O}_6(\text{OCH}_3)_{13}]^-$ (**1-TiV₅**), the most notable change in the voltammetric profile is the appearance of an additional reduction event located at $E_{1/2} = -2.07$ V (vs. Ag/Ag^+). Spectroelectrochemical analysis of a reduced solution of **1-TiV₅** confirms that this isolated redox event can be assigned to the reduction of titanium ($\text{Ti}^{\text{IV}} \rightarrow \text{Ti}^{\text{III}}$; Figure 3a) (*vide infra*). This event, combined with its nearest, vanadium-based oxidation, results in a V_{cell} of 2.30 V for **1-TiV₅**, marking a 44% increase from that reported for the hexavanadate derivative (1.6 V).⁵⁴ This observation highlights the ability of installation of d^0 metal centres to dramatically improve the V_{cell} of the Lindqvist cluster.

Recently we reported the synthesis of a dititanium-functionalized POV-alkoxide cluster, $[\text{Ti}^{\text{IV}}_2\text{V}_4\text{O}_5(\text{OCH}_3)_{14}]$ (**2-Ti₂V₄**, Figure 2a).⁵⁵ The CV of **2-Ti₂V₄** reveals a set of four redox events, spanning -2.10 V to 0.64 V (Figure 2b, Table 1). Open circuit potential measurements indicate zero current at -0.30 V, confirming that the $[\text{Ti}^{\text{IV}}_2\text{V}_4\text{O}_5]$ oxidation state distribution of **2-Ti₂V₄** falls between the widely spaced pairs of reduction and oxidation events. Thus, in analogy to **1-TiV₅**, we attribute the oxidation events ($E_{1/2} = 0.15, 0.64$ V) to successive, single-electron, vanadium-based processes ($\text{V}^{\text{IV}} \rightarrow \text{V}^{\text{V}}$). The two reduction events ($E_{1/2} = -1.58, -2.10$ V) are assigned to the

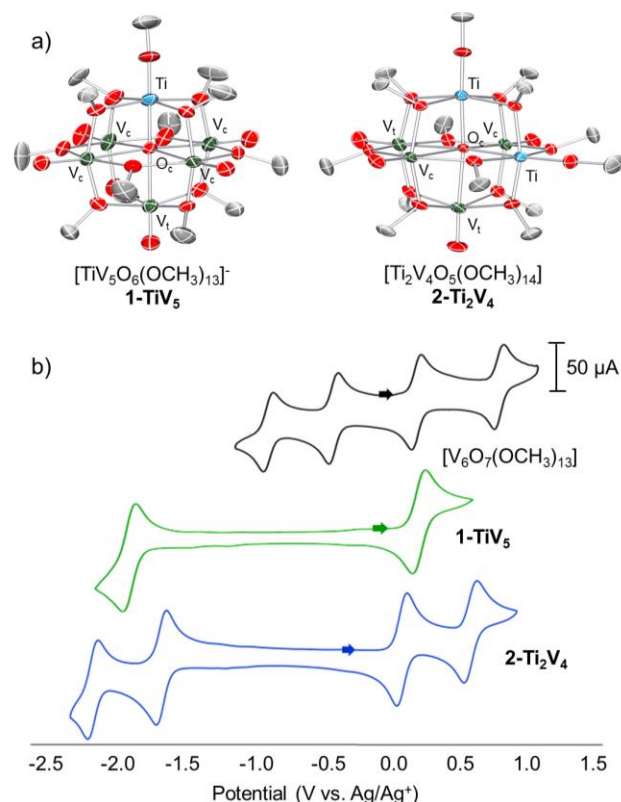


Figure 2. a) Molecular structures of **1-TiV₅** and **2-Ti₂V₄** shown with 50% probability ellipsoids. Hydrogen atoms and counter ions have been removed for clarity; b) CVs of $[\text{V}_6\text{O}_7(\text{OCH}_3)_{12}]$, **1-TiV₅**, and **2-Ti₂V₄**. Spectra collected in acetonitrile at a scan rate of 20 mV/s with 0.1 mM $[\text{NBu}_4][\text{PF}_6]$.

Table 1. Solubility and electrochemical parameters of complexes **1-TiV₅** and **2-Ti₂V₄**.

Complex	Solubility (M)	2 nd Ti ^{III} /Ti ^{IV} couple ^a	1 st Ti ^{III} /Ti ^{IV} couple ^a	1 st V ^{IV} /V ^V couple ^a	2 nd V ^{IV} /V ^V couple ^a
1-TiV₅	0.513	--	-2.07 (1.06)	0.23 (1.00)	--
2-Ti₂V₄	0.193	-2.10 (1.77)	-1.58 (1.12)	0.15 (1.05)	0.64 (0.99)

^a Standard potentials (measured vs. Ag/Ag⁺) identified using cyclic voltammetry at 20 mV/s of 5 mM solutions of each complex with 0.1 M [NBu₄][PF₆] supporting electrolyte in acetonitrile. Values in parentheses indicate ratios of the cathodic and anodic peak heights (i_c/i_a).

sequential reductions of the two titanium ions imbedded within the Lindqvist core (Ti^{IV}→Ti^{III}; Table 1). Collectively, the electrochemical profiles of **1-TiV₅** and **2-Ti₂V₄** demonstrate that heterometal incorporation has the ability to support not only an expansion of V_{cell} , but also an increase in the number of electrons stored by the charge carrier.

Anderson *et al.* have demonstrated that the combination of low- (V^{IV}) and high- (W^{VI}) valent metal centres can significantly expand V_{cell} for mixed-metal POMs in aqueous conditions.^{50, 56} To fully exploit the broad range of redox events afforded by two different metals, the authors attempted to translate their charge carrier, [SiV₃W₉O₄₀]⁷⁻, to organic solvent. While they note that the use of propylene carbonate significantly improves the separation between the vanadium oxidation and tungsten reduction events (to 1.7 V, from 0.8 V in the aqueous system), they observe a concurrent loss of electrochemical reversibility in the CV of this oxo-bridged cluster. In contrast, the CVs of **1-TiV₅** and **2-Ti₂V₄**, measured in acetonitrile, show cathodic to anodic peak height ratios (i_c/i_a)

near unity, suggesting that their redox chemistry is well-suited for nonaqueous electrochemical applications (Table 1).

Electrochemical stability: bulk electrolysis. For TiPOV-alkoxide clusters to serve as successful NRFB charge carriers, it is important that they demonstrate long-term, solution-state stability across all charge states accessed during battery cycling. To investigate the stability of **1-TiV₅** in its reduced and oxidized forms, bulk electrolysis was conducted at -2.10 V and 0.25 V, respectively (Figure S1). Electronic absorption spectroscopy was used to confirm the formation of the desired reduced and oxidized clusters (Figure 3a), as this technique has been demonstrated to be an effective tool for probing the oxidation state distributions of POV-alkoxide clusters.^{52-54, 57, 58} The absorption spectrum of the original cluster, **1-TiV₅**, shows two characteristic absorbance features: the first at 630 nm ($\epsilon = 60 \text{ M}^{-1}\text{cm}^{-1}$), assigned to a forbidden $d_{xy}(V^{IV}) \rightarrow d_{x^2-y^2}(V^{IV})$ excitation of the iso-valent, V^{IV}₅ POV-alkoxide scaffold; the second at 450 nm ($\epsilon = 579 \text{ M}^{-1}\text{cm}^{-1}$), attributed to charge transfer from a V^{IV} (d^1) centre to the Ti^{IV} (d^0) ion.⁵⁴ In the

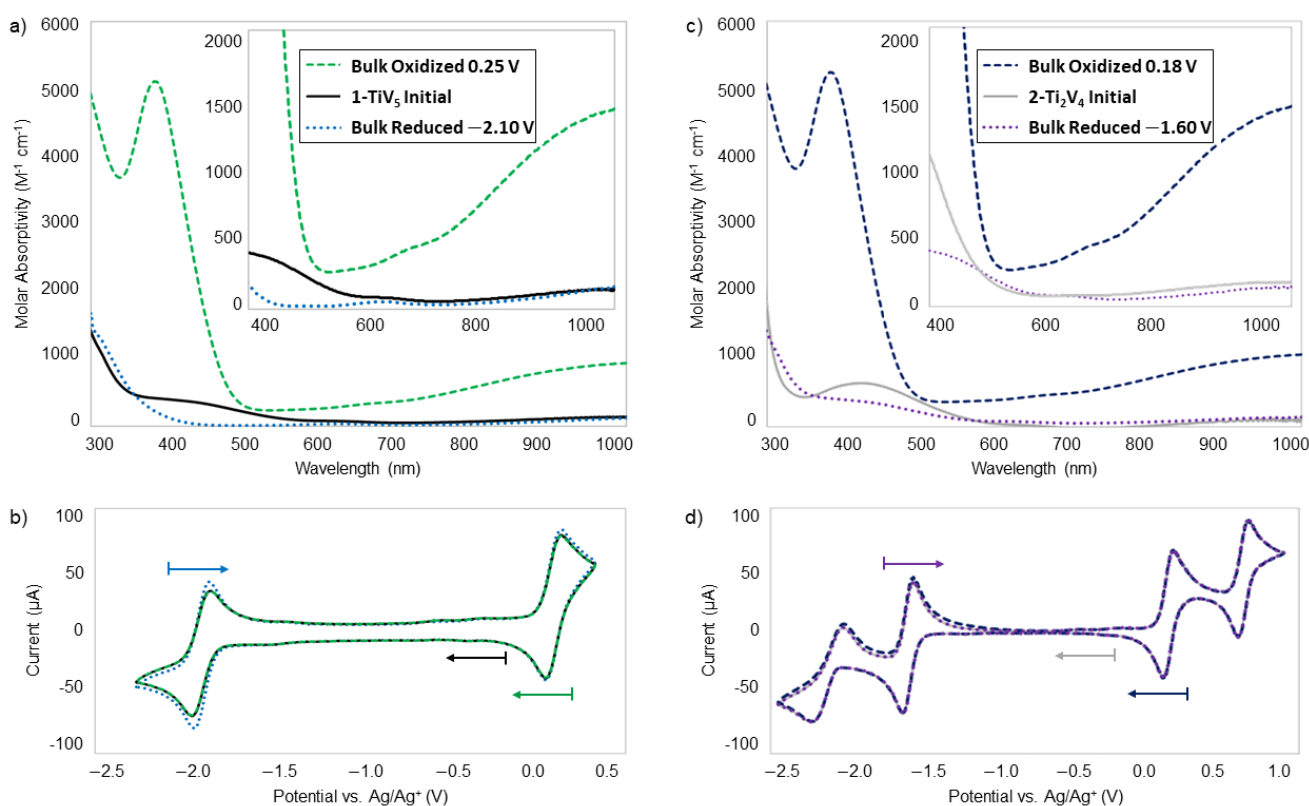


Figure 3. (a) Absorption spectra and (b) cyclic voltammograms of solutions of **1-TiV₅** before and after bulk oxidation and reduction. Similar spectra for **2-Ti₂V₄** are shown in (c) and (d). Cluster concentration were 5mM in acetonitrile with 0.1 M [NBu₄][PF₆] supporting electrolyte. Absorption spectra blanked with 0.1 M [NBu₄][PF₆] in acetonitrile. CV spectra are overlaid to compare i_p and $E_{1/2}$ values in the various charge states of the solutions.

spectrum of the reduced solution, the only observed feature is a weak absorption at 632 nm ($\epsilon = 51 \text{ M}^{-1}\text{cm}^{-1}$) indicating retention of the isovalent, V^{V} electronic configuration. The absence of an absorbance feature at 450 nm suggests reduction of the heterometal to Ti^{III} to form the reduced cluster, $[\text{Ti}^{\text{III}}\text{V}^{\text{V}}\text{O}_6(\text{OCH}_3)_{13}]^{2-}$. This reduction of **1-TiV₅** is accompanied by a colour change from brown-red to pale blue (Figure S2). In contrast, bulk oxidation of **1-TiV₅** resulted in a colour change to dark green. The absorption spectrum of the oxidized solution bears two absorptions located at 384 nm ($\epsilon = 5110 \text{ M}^{-1}\text{cm}^{-1}$) and 1000 nm ($\epsilon = 1381 \text{ M}^{-1}\text{cm}^{-1}$)—characteristic features of mixed-valent POV-alkoxide clusters. The transition at lower energies corresponds to an IVCT absorption between $d_{xy}(\text{V}^{\text{IV}}) \rightarrow d_{xy}(\text{V}^{\text{V}})$ orbitals, while the higher energy absorption is assigned to a $d_{xy}(\text{V}^{\text{IV}}) \rightarrow d_{x^2-y^2}(\text{V}^{\text{V}})$ excitation.^{52-54, 57, 58} Appearance of these features is therefore consistent with successful oxidation of a single vanadium centre within the Lindqvist core, from V^{IV} to V^{V} , to form the oxidized cluster, $[\text{Ti}^{\text{IV}}\text{V}^{\text{V}}\text{V}^{\text{V}}\text{O}_7(\text{OCH}_3)_{13}]^0$.

The resulting oxidized and reduced solutions were analyzed *via* CV to confirm that no cluster degradation occurred during bulk electrolysis (Figure 3b). No substantial changes were observed in peak potential or current response or for the CVs of the oxidized and reduced solutions, indicating quantitative conversion of **1-TiV₅** to its oxidized and reduced derivatives. The durability of complex **1-TiV₅** across all three charge states was assessed by monitoring the charged solutions using CV and electronic absorption spectroscopy (Figure S3). Over the course of one week, no evidence of degradation or self-discharge of the charge carrier was noted, indicating that **1-TiV₅** is stable across the staggering 2.3 V potential range suggested by the CV.

Similar bulk electrolysis experiments were conducted with complex **2-Ti₂V₄**. To determine the accessibility and stability of the five available charge states, reduction experiments were conducted at -1.60 V and -2.13 V to generate the mono- and di-anionic clusters, while oxidations at 0.18 V and 0.67 V were used to access the corresponding mono- and di-cationic species (Figure S4). Examining the UV-vis spectra of and CV the mono-cationic and mono-anionic solutions following bulk electrolysis

indicates successful formation of the singly reduced ($[\text{Ti}^{\text{III}}\text{Ti}^{\text{IV}}\text{V}^{\text{V}}\text{O}_5(\text{OCH}_3)_{14}]^-$) and oxidized ($[\text{Ti}^{\text{IV}}\text{V}^{\text{IV}}\text{V}^{\text{V}}\text{O}_5(\text{OCH}_3)_{14}]^+$) compounds (Figure 3c). However, attempts to generate the di-cationic ($[\text{Ti}^{\text{IV}}\text{V}^{\text{IV}}\text{V}^{\text{V}}\text{O}_5(\text{OCH}_3)_{14}]^{2+}$) and di-anionic ($[\text{Ti}^{\text{III}}\text{V}^{\text{IV}}\text{O}_5(\text{OCH}_3)_{14}]^{2-}$) derivatives were unsuccessful, evidenced by the significant changes in the electronic absorption spectra and CVs of these solutions when exposed to highly oxidizing and highly reducing potentials (Figure S5-S6).

Electronic absorption spectroscopy of the singly-reduced and oxidized solutions of **2-Ti₂V₄** unambiguously confirms the hypothesis that these accessible redox events are based in two different metal centres. Similar to the observed changes in the spectrum of **1-TiV₅** following reduction, the mono-reduced solution of **2-Ti₂V₄** shows a weak absorption at 632 nm ($\epsilon = 81 \text{ M}^{-1}\text{cm}^{-1}$) suggesting an isovalent, V^{V} electronic configuration (Figure 4c). Unlike reduced **1-TiV₅**, however, the mono-reduced solution of **2-Ti₂V₄** retains a feature corresponding to IVCT between V^{IV} and Ti^{IV} ions (430 nm). This results from retention of the Ti^{IV} electronic configuration in the second heteroatom, which supports continued IVCT between the $d^1 \text{V}^{\text{IV}}$ and $d^0 \text{Ti}^{\text{IV}}$ ions. Accordingly, the molar absorptivity of this absorbance in the reduced complex is decreased from that of neutral **2-Ti₂V₄** (from $\epsilon = 643 \text{ M}^{-1}\text{cm}^{-1}$ to $\epsilon = 367 \text{ M}^{-1}\text{cm}^{-1}$). The absorption spectrum of the singly oxidized solution of **2-Ti₂V₄** shows strong features at 382 nm ($\epsilon = 5244 \text{ M}^{-1}\text{cm}^{-1}$) and 1000 nm ($\epsilon = 1432 \text{ M}^{-1}\text{cm}^{-1}$), which, as discussed in the case of **1-TiV₅**, confirms successful oxidation of a vanadium ion from V^{IV} to V^{V} .

CVs of **2-Ti₂V₄** following electrolysis to the mono-cationic and -anionic charge states revealed no changes in current response or $E_{1/2}$ potentials, only a shift in open circuit potential (Figure 3d). Thus, there is no degradation of **2-Ti₂V₄** during conversion to its singly oxidized and reduced derivatives. Monitoring these solutions for one week using CV and electronic absorption spectroscopies revealed that both charge states were resistant to decomposition and self-discharge (Figure S7). This indicates that, although highly oxidizing or reducing environments yield cluster decomposition, **2-Ti₂V₄**

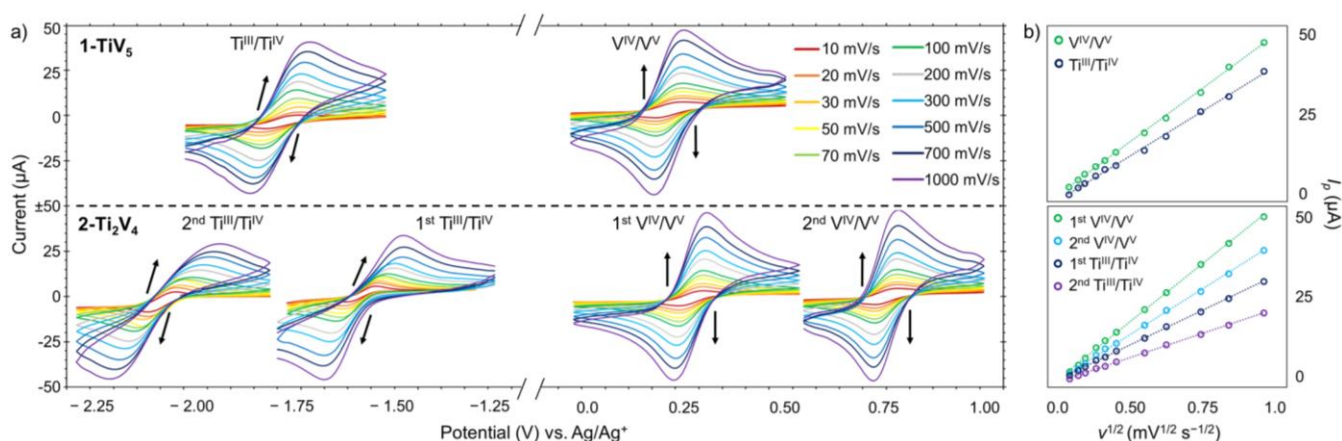


Figure 4. (a) Cyclic voltammograms of the isolated redox events **1-TiV₅** (top) and **2-Ti₂V₄** (bottom) at scan rates from 10-1000 mV s^{-1} . Acetonitrile solutions contained 5 mM active cluster with 0.1 M $[\text{NBu}_4][\text{PF}_6]$ supporting electrolyte. (b) Plots of the square root of scan rate versus the peak current for each redox event in **1-TiV₅** (top) and **2-Ti₂V₄** (bottom) demonstrating their linear relationship.

Table 2. Diffusion coefficients and heterogeneous electron transfer rate constants for each redox event in complexes **1-TiV₅** and **2-Ti₂V₄**.

Complex	2 nd Ti ^{III} /Ti ^{IV} couple		1 st Ti ^{III} /Ti ^{IV} couple		1 st V ^{IV} /V ^V couple		2 nd V ^{IV} /V ^V couple	
	<i>D</i> ₀ (cm ² /s)	<i>k</i> ₀ (cm/s)	<i>D</i> ₀ (cm ² /s)	<i>k</i> ₀ (cm/s)	<i>D</i> ₀ (cm ² /s)	<i>k</i> ₀ (cm/s)	<i>D</i> ₀ (cm ² /s)	<i>k</i> ₀ (cm/s)
1-TiV₅	--	--	5.8 × 10 ⁻⁶	7.7 × 10 ⁻³	4.4 × 10 ⁻⁶	3.1 × 10 ⁻²	--	--
2-Ti₂V₄	3.6 × 10 ⁻⁶	4.6 × 10 ⁻⁴	3.3 × 10 ⁻⁶	3.6 × 10 ⁻³	1.0 × 10 ⁻⁵	2.3 × 10 ⁻²	4.5 × 10 ⁻⁶	3.5 × 10 ⁻²

possesses long-term, solution state stability across a practical cell voltage of 1.73 V.

Electrokinetic parameters of TiPOV-alkoxide clusters. A successful RFB charge carrier must have sufficiently high electron transfer kinetics and diffusion coefficients to support complete charge transfer as electrolyte solutions are passed over a solid electrode surface.⁵⁹ To determine these values for **1-TiV₅** and **2-Ti₂V₄**, isolated CVs of each redox event were obtained at scan rates ranging from 10 to 1000 mV s⁻¹ (Figure 4a). Linear relationships between peak current (*i_p*) and the square root of the scan rate (*v*^{1/2}) were observed, indicating well-defined, mass-transfer limited processes for each electrochemical event (Figure 4b).^{60, 61} The Randles–Sevcik equation was used to determine diffusion coefficients for the redox series of the titanium-functionalized POV-alkoxide clusters (Table 2).^{16, 18, 62} These values are on the same order of magnitude as those of previously reported RFB charge carrier redox couples.^{59, 63, 64} For an EES device, wherein charge transfer is a mass-transport limited process (i.e., one with rapid charge transfer kinetics), the diffusion coefficients must be as high as possible to meet the performance targets for grid-scale energy storage.⁵⁹ The large diffusion coefficients of solution phase charge carriers, like **1-TiV₅** and **2-Ti₂V₄**, are a principle advantage of flow-based EES devices over solid-state systems.⁶⁵

Rapid heterogeneous electron transfer rate constants (*k*₀) for each redox event in **1-TiV₅** and **2-Ti₂V₄** were confirmed using the Nicholson method (Table 2).¹⁸ The peak separation (ΔE_p) was determined for each event, and plotted as a function of scan rate (Figure S8). The increase in ΔE_p at higher scan rates for the titanium-based reduction events of both **1-TiV₅** and **2-Ti₂V₄** indicates quasi-reversible kinetics for each of these reduction processes. In contrast, the ΔE_p is constant at all scan rates for the vanadium-based oxidation events, indicative of kinetically reversible electron transfer processes. The *k*₀ values for each of the titanium-based redox events in **1-TiV₅** and **2-Ti₂V₄** (~3.9 × 10⁻³ cm s⁻¹), are on par with those previously reported for charge carriers in non-aqueous energy storage.⁶³ The vanadium-based redox events, however, have rate constants which are notably high (~3.0 × 10⁻² cm s⁻¹), consistent with our observations for [V₆O₇(OR)₁₂] (R = CH₃, C₂H₅).⁵²

While the redox chemistry of vanadium has been frequently touted as superior to other metals,⁶² this alone does not account for the significant increase in charge transfer kinetics observed in the POV-alkoxide clusters, as compared to monometallic molecular complexes (e.g. V(acac)₃). Instead, we attribute this property to the Robin & Day Class II, delocalized electronic structure of homo- and heterometallic POV-alkoxide

clusters.⁶⁶ The cooperative electronic interaction between the vanadium ions facilitates electron transfer in and out of the system, with no significant changes to the molecular structure of the cluster core. The large heterogeneous electron transfer rate constants have positive implications for NRFB functionality, as voltage losses should be mitigated by rapid exchange of electron density. Given the direct relationship between faradaic current and rate constant, redox reactions with larger *k*₀ values, such as those observed in our POV-alkoxide clusters, will reach equilibrium more quickly, yielding battery cells with superior energy efficiencies as compared to other RFB charge carriers.

Solubility of TiPOV-alkoxide clusters in acetonitrile. In addition to electrochemical instability, low solubility in organic media is a major contributor to the limited success of previously reported electroactive materials for NRFBs. For POM-based charge carriers, the oxo-bridged, high-valent metal centres typically result in highly charged structures, which are challenging to dissolve in organic solvents. In contrast, the electron-donating, bridging alkoxide ligands of the POV-alkoxide series solubilize the complex through organic functionality and the stabilization of low charge states of the Lindqvist core. The solubilities of **1-TiV₅** and **2-Ti₂V₄** were determined using electronic absorption spectroscopy in 0.1 M MeCN solutions of tetrabutylammonium hexafluorophosphate ([NBu₄][PF₆]) (Figures S9-S10). These conditions were selected to mirror the relevant working conditions of a NRFB cell. Complex **1-TiV₅** was measured to have a solubility of 0.513 M, while **2-Ti₂V₄** possessed a solubility of 0.193 M (Table 1).

The solubilities of the TiPOV-alkoxide clusters mark significant improvements from our previously reported hexavanadate derivatives, [V₆O₇(OR)₁₂] (R = CH₃, *C_{active}* = 0.102 M; R = C₂H₅, *C_{active}* = 0.048 M), and exceed, or are on par with, some of the most soluble metal coordination compounds reported for NRFB applications.^{19, 24, 38} We attribute these increases in solubility to the presence of terminal alkoxide ligands of the titanium ions, as the incorporation of [Ti(OR)]³⁺ cations has been demonstrated to improve the solubility of Lindqvist polyoxomolybdate and -tungstate clusters.⁶⁷⁻⁶⁹ This, in conjunction with the increase in *V_{cell}*, suggests that **1-TiV₅** and **2-Ti₂V₄** could dramatically improve upon the theoretical volumetric energy densities of our previously reported hexavanadate clusters.

Membrane crossover of TiPOV-alkoxide clusters. In flow-based EES devices, the typical approach to exploiting the divergent redox properties of different metal centres is to generate an asymmetric cell, with two separate metal coordination

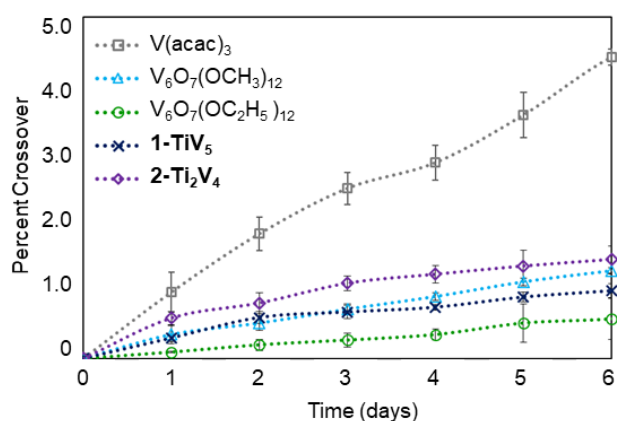


Figure 5. Percent crossover of POV-alkoxide clusters compared to that of V(acac)₃ over the course of 6 days.

complexes composing the anolyte and catholyte solutions.²³ However, membrane crossover in these asymmetric systems can result in irreversible decomposition of the active species, making frequent replacement of electrolyte solutions necessary for device functionality.^{17,62} A major advantage to the development of mixed metal symmetric charge carriers, like **1-TiV₅** and **2-Ti₂V₄**, is the opportunity to capitalize on the redox chemistry of two different transition metals, harnessed within a single molecule. This ability to use a single molecule as both anolyte and catholyte significantly mitigates the degradative effects of crossover. However, in the event of species crossover, charge compensation is required to re-equilibrate the cell, which can reduce the overall energy efficiency.⁶³ As such, even in symmetric cell designs, minimizing the ability of active species to pass through a membrane is an important consideration for long-term RFB efficiency.

Our previous work with hexavanadate POV-alkoxide clusters established that these bulky, three-dimensional frameworks exhibit minimal crossover over the course of several days.⁵² To extrapolate these investigations to the heterometallic scaffolds, we measured crossover for the titanium-functionalized POV-alkoxide clusters, **1-TiV₅** and **2-Ti₂V₄**. We quantified the fraction of active species crossover through the anion exchange membrane (AMI-7001) of the H-cell using electronic absorption spectroscopy (Figure S11). From these experiments, we observe that the membrane permeation of **1-TiV₅** and **2-Ti₂V₄** is similarly low, in analogy to values observed for the hexavanadate assemblies (Figure 5). The percentage traces of species crossover are plotted against that observed for V(acac)₃, a compound considered resistant to membrane crossover in comparison to other metal coordination complexes.¹⁶ We credit the minimal crossover observed for **1-TiV₅** and **2-Ti₂V₄** to the bulky nature of the POV-alkoxide framework. Analogous approaches to the prevention of membrane crossover have been demonstrated effective for redox-active organic oligomers, through increasing the steric bulk of a charge carrier.^{37, 70} To date, however, these organic systems lack the requisite stability for use in long-term use in energy storage devices. Our chemically robust assembled POV-alkoxide scaffolds combine the stability of metal-based systems with the

bulky nature of these oligomers, resulting in a charge carrier that is uniquely resistant to membrane crossover.

Theoretical Energy Density. The stability of the TiPOV-alkoxide clusters, coupled with their resistance to membrane crossover, suggests that these heterometallic complexes can serve as charge carriers in symmetric schematics, capable of transferring one electron at each electrode. Therefore, using Eq. 1, we can calculate the theoretical volumetric energy density for each cluster. A V_{cell} of 2.30 V and solubility of 0.513 M yields an energy density of 57 kJ L⁻¹ for **1-TiV₅**, representing a 400% improvement over that of [V₆O₇(OCH₃)₁₂] (14.2 kJ L⁻¹) and a 740% increase over [V₆O₇(OC₂H₅)₁₂] (7.7 kJ L⁻¹).⁵² While the CV of **2-Ti₂V₄** suggests a V_{cell} of 2.74 V, the stability of this cluster limits the practical cell voltage to 1.73 V. This, in conjunction with a solubility of 0.193 M, gives a theoretical energy density of 16.1 kJ L⁻¹. These improvements in energy density for the TiPOV-alkoxide clusters render our systems competitive with the highest reported values for metal-based charge carriers in NRFB applications.^{13, 16, 18, 19, 21, 22, 24, 38}

Extended cycling of TiPOV-alkoxide clusters. The physicochemical properties of the TiPOV-alkoxides motivated continued analyses as NRFB charge carriers. As such, we transitioned from fundamental electrochemical studies to proof-of-concept analyses through H-cell charge-discharge cycling experiments. In these experiments, 5 mM acetonitrile solutions of **1-TiV₅**, with 0.1 M [NBu₄][PF₆] supporting electrolyte, were used as both the anolyte and catholyte in an H-cell, separated by an anion exchange membrane (AMI-7001). Carbon mesh electrodes (2 × 1 × 0.5 cm) were placed in the anolyte and catholyte compartments with stirring and galvanostatically charged ($i = 0.15$ mA/cm²) until they reached the set cut-off potential, 2.7 V. The cut-off potential was set higher than the V_{cell} of **1-TiV₅** to compensate for the inherent overpotential associated with H-cell design. Once the 2.7 V cut-off was reached, solutions were galvanostatically discharged to 0.1 V ($i = 0.015$ mA/cm²). The lower discharge current density was selected to ensure complete cell discharge.

Solutions of **1-TiV₅** were cycled 20 times (trace of cycles 3-7 is shown in Figure 6a, all 20 cycles can be seen in Figure S12). In the voltage trace, a clear charging plateau is observed at 2.3 V, in agreement with the V_{cell} of **1-TiV₅** determined by CV. The coulombic efficiency in this system stays at ~91% throughout cycling, indicative of quantitative electron transfer to and from the cluster (Figure 6b, Figure S13). To determine the stability of the charge carrier under charge-discharge conditions, the electrolyte solutions were monitored by CV (Figure 6c). The consistency in spectra indicates that cluster degradation does not occur during cycling experiments. The stable electron storage using **1-TiV₅** as a charge carrier marks the highest potential we are aware of for multimetallic redox systems in symmetric NRFBs.^{13, 16, 18, 19, 21, 22, 24, 38, 50, 52, 71}

Similar charge-discharge experiments were conducted for **2-Ti₂V₄**. Given the instability of the dititanium-functionalized POV-alkoxide cluster under highly oxidizing and reducing conditions, charge-discharge cycling was conducted at a lower cut-off

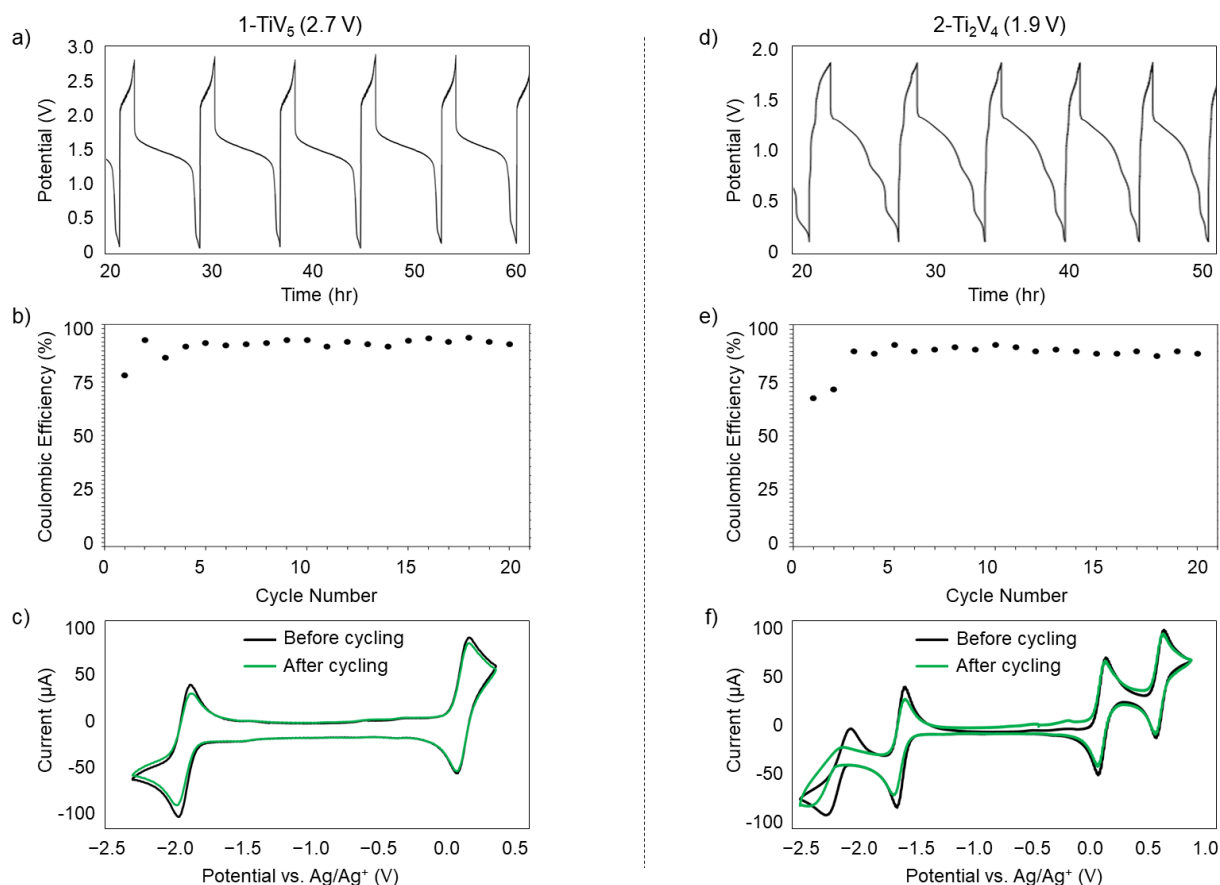


Figure 6. (a) Voltage trace of cycles 2-5 in charge-discharge cycling of **1-TiV₅**. (b) Coulombic efficiencies over 20 charge-discharge cycles of **1-TiV₅**. (c) Cyclic voltammograms of solutions before and after charge-discharge cycling overlaid to demonstrate the stability of compounds during cycling. Figures (d) (e) and (f) show similar characterizations for charge-discharge cycling of **2-Ti₂V₄**. Charge-discharge experiments were conducted in an H-cell separated by an anion exchange membrane (AMI-7001). 5 mM acetonitrile solutions of each active species with 0.1 M [NBu₄][PF₆] supporting electrolyte were used as anolyte and catholyte. Galvanostatic conditions were used for charging ($i = 0.15 \text{ mA/cm}^2$) and discharging ($i = 0.015 \text{ mA/cm}^2$).

potential, 1.9 V, to limit cycling to one electron at each electrode. Figure 6d shows the trace of cycles 3-7 from this experiment, while all cycles can be viewed in Figure S14. The coulombic efficiency throughout cycling was approximately 89% (Figure 6e, Figure S15). CV of the electrolyte solutions following charge-discharge showed only slight changes in current response, confirming the stability of **2-Ti₂V₄** (Figure 6f).

Unlike the voltage trace of **1-TiV₅**, the trace of the cycling experiment of **2-Ti₂V₄** does not exhibit clear charging and discharging plateaus. Similar traces have been attributed by others to poor electrochemical reversibility of the charge carrier, however we note that the reversibility of the redox events of **2-Ti₂V₄** is similar to those of **1-TiV₅** (Table 2). This observation suggests that additional factors contribute to the anomalous charge-discharge trace. Comparison of the CVs of charge carrier solutions before and after charge-discharge experiments demonstrate the stability of both clusters during cycling, removing decomposition as a potential source of the observed perturbations. To address the differences, we examined the diffusion coefficients and electron transfer rate kinetics of the redox processes for each system (Table 2). In doing so, we note that D_0 and k_0 values of reduction and oxidation events of **2-Ti₂V₄** differ by an order of magnitude ($D_0 = 3.3 \times 10^{-6}$ vs. $1.0 \times 10^{-5} \text{ cm}^2 \text{ s}^{-1}$; $k_0 = 3.6 \times 10^{-3}$ vs. $2.3 \times 10^{-2} \text{ cm}^2$

s^{-1}). In contrast, the values measured for the reduction and oxidation of **1-TiV₅** are similar in size ($D_0 = 5.8 \times 10^{-6}$ vs. $4.4 \times 10^{-6} \text{ cm}^2 \text{ s}^{-1}$; $k_0 = 7.7 \times 10^{-3}$ vs. $3.1 \times 10^{-2} \text{ cm}^2 \text{ s}^{-1}$). As such, we hypothesized that the differences in cycling traces to this confluence in diffusion kinetics.

Intrigued by this observation, we compared our system to a recently reported stable asymmetric system, which invokes the redox chemistry of two distinct metal phosphate complexes, $[\text{M}(\text{P}_3\text{O}_9)_2]^{3-/4-}$ ($\text{M} = \text{Co}, \text{V}$) as the anode and cathode.²³ In analogy to the charge-discharge profile of **2-Ti₂V₄**, the trace of the Co/V system exhibits slight perturbations in charging and discharging plateaus. Comparison of the diffusion coefficients and electron transfer rate constants reported for $[\text{Co}^{\text{II/III}}(\text{P}_3\text{O}_9)_2]^{3-/4-}$ and $[\text{V}^{\text{II/III}}(\text{P}_3\text{O}_9)_2]^{3-/4-}$ reveals a disparity in the values of the electrokinetic parameters reported for the anolyte ($D_0 = 1.8 \times 10^{-8} \text{ cm}^2 \text{ s}^{-1}$; $k_0 = 2.8 \times 10^{-5} \text{ cm}^2 \text{ s}^{-1}$) and catholyte ($D_0 = 2.3 \times 10^{-6} \text{ cm}^2 \text{ s}^{-1}$; $k_0 = 1.0 \times 10^{-3} \text{ cm}^2 \text{ s}^{-1}$). This supports the role of mismatched diffusion coefficients and electron transfer rate constants of multiple metal centres in the observed disruptions in the charge-discharge voltage trace. Moving forward, the differences in these properties must be considered when designing a multimetallic charge carrier.

Conclusions

In this work, we report a synthetic inorganic approach for improving the physicochemical properties of multimetallic charge carriers with relevance to their volumetric energy density. Collectively, increases in solubility and cell voltage for **1-TiV₅** and **2-Ti₂V₄** result in significant improvements of the energy storage capabilities of these heterometallic clusters over their hexavanadate congeners. The superb electrokinetic properties and stability of the multimetallic assemblies, combined with their ability to function in a symmetric cell, strongly advocates for their consideration as efficient NRFB charge carriers.

The installation of a second *d*⁰ heterometal shows promise for future charge carrier design, as this molecular modification not only increases the working potential of the system, but also creates the possibility for multielectron storage at each electrode. Although current charge-discharge cycling of **2-Ti₂V₄** demonstrates stability for the system only when limited to cycling one electron at each electrode, our previous work with POV-alkoxide clusters as NRFB charge carriers has established that ligand modification of these systems can improve the stability of highly reducing and oxidizing events.⁵² Ongoing investigations are focused on the generation of a stable heterometallic frameworks that can facilitate multielectron transfer, with an ultimate goal of identifying self-assembled, energy-dense materials for NRFB applications.

Conflicts of interest

There are no conflicts to declare

Acknowledgements

The authors acknowledge Timothy R. Cook and Anjula M. Kosswattaarachchi for their helpful discussions. The authors would like to thank the University of Rochester for financial support. L. E. V. is supported by the National Science Foundation Graduate Research Fellowship Program (DGE-1419118)

References

- Z. Yang, J. Zhang, M. C. W. Kintner-Meyer, X. Lu, D. Choi, J. P. Lemmon and J. Liu, *Chemical Reviews*, 2011, **111**, 3577-3613.
- B. Dunn, H. Kamath and J.-M. Tarascon, *Science*, 2011, **334**, 928-935.
- C. Ponce de León Albarrán, Á. Frías Ferrer, J. González García, D. A. Szánto and F. C. Walsh, DOI: 10.1016/j.jpowsour.2006.02.095.
- T. Nguyen and R. F. Savinell, *The Electrochemical Society Interface*, 2010, **19**, 54-56.
- Q. Huang and Q. Wang, *ChemPlusChem*, 2015, **80**, 312-322.
- P. Alotto, M. Guarnieri and F. Moro, *Renewable and Sustainable Energy Reviews*, 2014, **29**, 325-335.
- Y. Wang and H. Zhou, *Energy & Environmental Science*, 2016, **9**, 2267-2272.
- L. Zhang, C. Zhang, Y. Ding, K. Ramirez-Meyers and G. Yu, *Joule*, 2017, **1**, 623-633.
- Z. Changkun, D. Yu, Z. Leyuan, W. Xuelan, Z. Yu, Z. Xiaohong and Y. Guihua, *Angewandte Chemie*, 2017, **129**, 7562-7567.
- J. Li, L. Yang, S. Yang and Y. Lee Jim, *Advanced Energy Materials*, 2015, **5**, 1501808.
- Q. Huang, J. Yang, C. B. Ng, C. Jia and Q. Wang, *Energy & Environmental Science*, 2016, **9**, 917-921.
- A. M. Kosswattaarachchi and T. R. Cook, *Journal of The Electrochemical Society*, 2018, **165**, A194-A200.
- K. Gong, Q. Fang, S. Gu, S. F. Y. Li and Y. Yan, *Energy & Environmental Science*, 2015, **8**, 3515-3530.
- R. M. Darling, K. G. Gallagher, J. A. Kowalski, S. Ha and F. R. Brushett, *Energy & Environmental Science*, 2014, **7**, 3459-3477.
- M. H. Chakrabarti, R. A. W. Dryfe and E. P. L. Roberts, *Electrochimica Acta*, 2007, **52**, 2189-2195.
- Q. Liu, A. E. S. Sleightholme, A. A. Shinkle, Y. Li and L. T. Thompson, *Electrochemistry Communications*, 2009, **11**, 2312-2315.
- Q. Liu, A. A. Shinkle, Y. Li, C. W. Monroe, L. T. Thompson and A. E. S. Sleightholme, *Electrochemistry Communications*, 2010, **12**, 1634-1637.
- A. E. S. Sleightholme, A. A.; Qinghua L.; Yongdan L.; Monroe, C. W.; and Thompson, L. T., *Journal of Power Sources*, 2011, **196**, 5742-5745.
- P. J. Cabrera, X. Yang, J. A. Suttill, R. E. M. Brooner, L. T. Thompson and M. S. Sanford, *Inorganic Chemistry*, 2015, **54**, 10214-10223.
- P. J. Cabrera, X. Yang, J. A. Suttill, K. L. Hawthorne, R. E. M. Brooner, M. S. Sanford and L. T. Thompson, *The Journal of Physical Chemistry C*, 2015, **119**, 15882-15889.
- J. Mun, M.-J. Lee, J.-W. Park, D.-J. Oh, D.-Y. Lee and S.-G. Doo, *Electrochemical and Solid-State Letters*, 2012, **15**, A80-A82.
- P. J. Cappillino, H. D. Pratt, N. S. Hudak, N. C. Tomson, T. M. Anderson and M. R. Anstey, *Advanced Energy Materials*, 2014, **4**, 1300566.
- J. M. Stauber, S. Zhang, N. Gvozdzik, Y. Jiang, L. Avena, K. J. Stevenson and C. C. Cummins, *Journal of the American Chemical Society*, 2018, **140**, 538-541.
- C. S. Sevov, S. L. Fisher, L. T. Thompson and M. S. Sanford, *Journal of the American Chemical Society*, 2016, **138**, 15378-15384.
- T. Yamamura, Y. Shiokawa, H. Yamana and H. Moriyama, *Electrochimica Acta*, 2002, **48**, 43-50.
- J.-H. Kim, K. J. Kim, M.-S. Park, N. J. Lee, U. Hwang, H. Kim and Y.-J. Kim, *Electrochemistry Communications*, 2011, **13**, 997-1000.
- D. Zhang, H. Lan and Y. Li, *Journal of Power Sources*, 2012, **217**, 199-203.
- A. M. Kosswattaarachchi, A. E. Friedman and T. R. Cook, *ChemSusChem*, 2016, **9**, 3317-3323.
- C. S. Sevov, R. E. M. Brooner, E. Chénard, R. S. Assary, J. S. Moore, J. Rodríguez-López and M. S. Sanford, *Journal of the American Chemical Society*, 2015, **137**, 14465-14472.
- J. Winsberg, C. Stolze, S. Muench, F. Liedl, M. D. Hager and U. S. Schubert, *ACS Energy Letters*, 2016, **1**, 976-980.
- X. Wei, W. Xu, J. Huang, L. Zhang, E. Walter, C. Lawrence, M. Vijayakumar, W. A. Henderson, T. Liu, L. Cosimbescu, B. Li, V. Sprenkle and W. Wang, *Angewandte Chemie International Edition*, 2015, **54**, 8684-8687.

32. A. P. Kaur, N. E. Holubowitch, S. Ergun, C. F. Elliott and S. A. Odum, *Energy Technology*, 2015, **3**, 476-480.
33. X. Wei, W. Duan, J. Huang, L. Zhang, B. Li, D. Reed, W. Xu, V. Sprenkle and W. Wang, *ACS Energy Letters*, 2016, **1**, 705-711.
34. J. Winsberg, T. Hagemann, S. Muench, C. Friebe, B. Häupler, T. Janoschka, S. Morgenstern, M. D. Hager and U. S. Schubert, *Chemistry of Materials*, 2016, **28**, 3401-3405.
35. G. Nagarjuna, J. Hui, K. J. Cheng, T. Lichtenstein, M. Shen, J. S. Moore and J. Rodriguez-López, *Journal of the American Chemical Society*, 2014, **136**, 16309-16316.
36. S. H. Oh, C. W. Lee, D. H. Chun, J. D. Jeon, J. Shim, K. H. Shin and J. H. Yang, *Journal of Materials Chemistry A*, 2014, **2**, 19994-19998.
37. K. H. Hendriks, S. G. Robinson, M. N. Braten, C. S. Sevov, B. A. Helms, M. S. Sigman, S. D. Minter and M. S. Sanford, *ACS Central Science*, 2018, **4**, 189-196.
38. J. A. Suttill, J. F. Kucharyson, I. L. Escalante-Garcia, P. J. Cabrera, B. R. James, R. F. Savinell, M. S. Sanford and L. T. Thompson, *Journal of Materials Chemistry A*, 2015, **3**, 7929-7938.
39. X. Xing, D. Zhang and Y. Li, *Journal of Power Sources*, 2015, **279**, 205-209.
40. G. M. Duarte, J. D. Braun, P. K. Giesbrecht and D. E. Herbert, *Dalton Transactions*, 2017, **46**, 16439-16445.
41. M. T. Pope and A. Müller, *Angewandte Chemie International Edition in English*, 1991, **30**, 34-48.
42. D. E. Katsoulis, *Chemical Reviews*, 1998, **98**, 359-388.
43. D.-L. Long, E. Burkholder and L. Cronin, *Chemical Society Reviews*, 2007, **36**, 105-121.
44. Y.-F. Song and R. Tsunashima, *Chemical Society Reviews*, 2012, **41**, 7384-7402.
45. N. L. O. Gunn, D. B. Ward, C. Menelaou, M. A. Herbert and T. J. Davies, *Journal of Power Sources*, 2017, **348**, 107-117.
46. D. B. Ward, N. L. O. Gunn, N. Uwigena and T. J. Davies, *Journal of Power Sources*, 2018, **375**, 68-76.
47. Y. Ji, L. Huang, J. Hu, C. Streb and Y.-F. Song, *Energy & Environmental Science*, 2015, **8**, 776-789.
48. N. Kawasaki, H. Wang, R. Nakanishi, S. Hamanaka, R. Kitaura, H. Shinohara, T. Yokoyama, H. Yoshikawa and K. Awaga, *Angewandte Chemie International Edition*, 2011, **50**, 3471-3474.
49. H. D. Pratt III and T. M. Anderson, *Dalton Transactions*, 2013, **42**, 15650-15655.
50. H. D. Pratt, N. S. Hudak, X. Fang and T. M. Anderson, *Journal of Power Sources*, 2013, **236**, 259-264.
51. J.-J. J. Chen and M. A. Barteau, *Industrial & Engineering Chemistry Research*, 2016, **55**, 9857-9864.
52. L. E. VanGelder, A. M. Kosswattaarachchi, P. L. Forrestel, T. R. Cook and E. M. Matson, *Chemical Science*, 2018, **9**, 1692-1699.
53. F. Li, L. E. VanGelder, W. W. Brennessel and E. M. Matson, *Inorganic Chemistry*, 2016, **55**, 7332-7334.
54. L. E. VanGelder, W. W. Brennessel and E. M. Matson, *Dalton Transactions*, 2018, **47**, 3698-3704.
55. L. E. F. VanGelder, P. L.; Brennessel, W. W.; Matson, E. M., *Chemical Communications. Accepted*.
56. H. D. Pratt, W. R. Pratt, X. Fang, N. S. Hudak and T. M. Anderson, *Electrochimica Acta*, 2014, **138**, 210-214.
57. F. Li, S. H. Carpenter, R. F. Higgins, M. G. Hitt, W. W. Brennessel, M. G. Ferrier, S. K. Cary, J. S. Lezama-Pacheco, J. T. Wright, B. W. Stein, M. P. Shores, M. L. Neidig, S. A. Kozimor and E. M. Matson, *Inorganic Chemistry*, 2017, **56**, 7065-7080.
58. C. Daniel and H. Hartl, *Journal of the American Chemical Society*, 2009, **131**, 5101-5114.
59. B. Yang, L. Hooper-Burkhardt, F. Wang, G. K. Surya Prakash and S. R. Narayanan, *Journal of The Electrochemical Society*, 2014, **161**, A1371-A1380.
60. K. J. Vetter, *Electrochemical Kinetics, Theoretical Aspects*, Academic Press, New York, NY, 1 edn., 1967.
61. J. F. Walling, *Journal of Chemical Education*, 1968, **45**, A142.
62. A. A. Shinkle, A. E. S. Sleightholme, L. T. Thompson and C. W. Monroe, *Journal of Applied Electrochemistry*, 2011, **41**, 1191-1199.
63. A. Z. Weber, M. M. Mench, J. P. Meyers, P. N. Ross, J. T. Gostick and Q. Liu, *Journal of Applied Electrochemistry*, 2011, **41**, 1137.
64. Y. Ding, Y. Zhao, Y. Li, J. B. Goodenough and G. Yu, *Energy & Environmental Science*, 2017, **10**, 491-497.
65. P. P. Prosini, M. Lisi, D. Zane and M. Pasquali, *Solid State Ionics*, 2002, **148**, 45-51.
66. M. B. Robin and P. Day, in *Advances in Inorganic Chemistry and Radiochemistry*, eds. H. J. Emeléus and A. G. Sharpe, Academic Press, 1968, vol. 10, pp. 247-422.
67. W. Clegg, M. R. J. Elsegood, R. J. Errington and J. Havelock, *Journal of the Chemical Society, Dalton Transactions*, 1996, DOI: 10.1039/DT9960000681, 681-690.
68. L. Coyle, P. S. Middleton, C. J. Murphy, W. Clegg, R. W. Harrington and R. J. Errington, *Dalton Transactions*, 2012, **41**, 971-981.
69. T. M. Che, V. W. Day, L. C. Francesconi, M. F. Fredrich, W. G. Klemperer and W. Shum, *Inorganic Chemistry*, 1985, **24**, 4055-4062.
70. S. E. Doris, A. L. Ward, A. Baskin, P. D. Frischmann, N. Gavvalapalli, E. Chénard, C. S. Sevov, D. Prendergast, J. S. Moore and B. A. Helms, *Angewandte Chemie International Edition*, 2017, **56**, 1595-1599.
71. J.-J. J. Chen and M. A. Barteau, *Journal of Energy Storage*, 2017, **13**, 255-261.

Table of Contents Entry: Heterometal functionalization within a polyoxovanadate-alkoxide cluster significantly increases the solubility and cell voltage, highlighting design strategies for non-aqueous, energy dense charge carriers.

